Journal of Molecular Liquids 379 (2023) 121735

Contents lists available at ScienceDirect

Journal of Molecular Liquids

journal homepage: www.elsevier.com/locate/molliq

Chitosan-based hydrogels obtained via photoinitiated click polymer IPN reaction

Pablo Sánchez-Cid [a,*], Alberto Romero [a], M.J. Díaz [b], M.V. de-Paz [c], Víctor Perez-Puyana [a]

[a] Departamento de Ingeniería Química, Facultad de Química, Universidad de Sevilla, 41012 Sevilla, Spain
[b] Pro2TecS—Chemical Process and Product Technology Research Center, Departamento de Ingeniería Química, Campus de "El Carmen", Universidad de Huelva, 21071 Huelva, Spain
[c] Departamento de Química Orgánica y Farmacéutica, Facultad de Farmacia, Universidad de Sevilla, 41012 Sevilla, Spain

ARTICLE INFO

Article history:
Received 27 January 2023
Revised 16 March 2023
Accepted 24 March 2023
Available online 29 March 2023

Keywords:
Chitosan
interpenetrated polymer network (IPN)
Click chemistry
Photo-polymerization
Rheology

ABSTRACT

Chitosan (CTS) is a polysaccharide with a wide variety of applications in the biomedical field, owing to its outstanding disinfectant properties, biocompatibility and biodegradability, but with limited mechanical properties. The proposed strategy to improve CTS-based hydrogel properties in this study is the formation of a semi-interpenetrating polymer network (semi-IPN). In this way, a photo-initiated radical click reaction was proposed to obtain a synthetic polymer, whose components were included in a CTS solution, resulting in the semi-IPN network after UV illumination. Different crosslinking degrees (CD) and CTS/polymer ratios were evaluated through rheological characterization, along with an assessment of both variables based on an experimental model design, obtaining that, for every CTS/polymer ratio, intermediate values of CD (8 %) offered the best rheological properties. In addition, chemical and microstructural characterization were carried out for selected hydrogels, obtaining consistent results according to rheological characterization, as the 1/1 CTS/polymer ratio with CD 8 % hydrogel displayed the most homogeneous pore size and distribution, consequently leading to the best rheological performance.

1. Introduction

Hydrogels are networks of hydrophilic polymers that can absorb thousands of times their dry weight of water without losing their structural integrity [1]. Due to this property, they are suitable candidates for several biomedical applications, such as tissue engineering [2], drug delivery [3] and wound dressing, as they can provide water to the wound area and therefore help to maintain a moist environment, consequently enhancing wound healing [4]. Hydrogels can be classified into two different types depending on the nature of intermolecular interactions between polymeric chains: 1) physical hydrogels, where crosslinking between chains is due to non-permanent physical bonds, such as Van der Waals interactions or hydrogen bonds, and 2) chemical hydrogels, whose crosslinking occurs due to covalent bonds, which are stronger [5,6].

Hydrophilic polymers (natural or synthetic), such as PVA [7], collagen/gelatin [8,9] or alginate [10], for example, are the most suitable materials for hydrogel fabrication, as they contain polar functional groups such as hydroxyl, carboxyl or amino groups that make them soluble or swelled by water [11]. Among them, chitosan is a well-known and widely used biopolymer for hydrogel crafting, due to its structure, versatility and properties, such as an excellent biocompatibility, biodegradability, low toxicity, cytocompatibility and mucoadhesiveness, as well as its anti-inflammatory, antibacterial, antifungal and wound-healing activities [12]. These properties have motivated a plethora of applications using chitosan. It is composed of repetitive units of D-glucosamine and *N*-acetyl-D-glucosamine connected by β-(1,4) linkages and randomly distributed. Chitosan is obtained from partial deacetylation of chitin, which is the most abundant natural amino polysaccharide in the world [13].

Chitosan-based hydrogels can be fabricated only by crosslinking of pure chitosan (homopolymer), or by chitosan combined with a second polymer (copolymeric), by either chemical or physical crosslinking. Each of these strategies may have an important impact on different properties, so it is possible to tune the chitosan-based hydrogels properties, by employing/investigating different strategies and materials [14]. However, even though chitosan is one of the best candidates for hydrogel formation, there are still several challenges to overcome, for example, the limitations of the characteristic properties due to the different interactions of fabricated hydrogel that hinder the applications of the chitosan-based gels or the need to develop fast-acting hydrogels with excellent mechanical strength [15,16].

* Corresponding author.
E-mail address: psanchezcid@us.es (P. Sánchez-Cid).

https://doi.org/10.1016/j.molliq.2023.121735
0167-7322/

Introducing interpenetrating polymer network (IPN) structures is an effective way to improve the mechanical performance of hydrogels and also increase porosity, enhance swelling behavior and improve cell adhesion [17]. In IPN hydrogels, each polymer forms a crosslinked network that is entangled with another polymer network [18]. These are unique "alloys" of crosslinked polymers in which at least one network is synthesized and/or crosslinked in the presence of the other, with no covalent bonds between them, in which both polymers cannot be separated unless chemical bonds are broken [19,20]. The combination of the polymers must effectively produce an advanced multicomponent polymeric system, with a new profile [21]. According to the chemistry of preparation, IPN hydrogels can be classified as: (i) simultaneous IPN, when the precursors of both networks are mixed, resulting in the formation of the two networks at the same time, or (ii) sequential IPN, typically performed by swelling of a single-network hydrogel into a solution containing the mixture of monomer, initiator and activator, with or without crosslinker [19,20]. With respect to their structures, IPN hydrogels can be classified as: (i) IPNs or full-IPNs, which are polymer matrices comprising two crosslinked networks interlaced on a molecular scale, or (ii) semi-IPNs, which are matrices comprising only one crosslinked network, in which the linear or branched polymer penetrates the network on a molecular scale [20,22]. Thus, IPN hydrogels offer the possibility of combining different polymers, such as two synthetic polymers, two biopolymers or even a combination of a biopolymer and a synthetic polymer, making use of the biocompatibility and hydrophilicity of the former and the mechanical and structural properties of the latter [22].

Synthetic polymers can be obtained and synthesized by many different processes and routes. Sharpless et al. [23] described a new concept for conducting highly selective organic reactions that do not yield side products and result in heteroatom-linked molecular systems with high efficiency under a variety of mild conditions, using eco-friendly solvent and synthesis processes [24]. Thus, several efficient reactions that meet these conditions and are capable of producing a wide variety of synthetic molecules and organic materials have been grouped accordingly under the term "click reactions". Highly efficient reactions of thiols with reactive carbon–carbon double bonds (alkenes) have been widely studied [25]. Thiol-ene click chemistry is a radical-mediated reaction that adds thiol groups to double bonds. This reaction has been shown to be highly efficient and tolerant to different functional groups [26]. They are considered "clickable" due to their high efficiency and selectivity. These reactions can take place under mild conditions in aqueous media with non-toxic byproducts. Thiol-ene reactions occur by two different routes or mechanisms: 1) a nucleophilic thiol-type Michael addition, and 2) a radically mediated thiol-ene reaction [27,28]. Thiol-ene reactions mediated by a radical mechanism can be initiated thermally or photochemically. Specifically, photo-initiated thiol-ene reactions are frequently used for the synthesis of hydrogel networks for biomedical applications such as injectables, tissue-regenerative hydrogels, and drug delivery systems, as well as in the synthesis of drugs per se, wound dressing and scaffolds for tissue engineering [27,29,30].

To obtain polymers via photo-initiated thiol-ene reactions, solutions containing the precursors with photo-reactive groups are prepared and subsequently irradiated with UV or visible light. Thus, a small amount of radical initiator is generated, which leads to the formation of the reactive thiyl radical (Fig. 1) [31]. After initiation, the reaction continues, with the thiyl radical on the alkene being attacked to form a new carbon radical. This carbon radical reacts with another thiol monomer, thus a thioether and a new thiyl radical are formed [32,33], which allow for the propagation to continue through a stepwise polymerization procedure, as is shown in the black cycle presented in Fig. 1.

Therefore, the main objective of this work is the development of chitosan-based IPN hydrogels. The novelty of this study is the synthesis of polymeric chains by photoinitiated click reactions between a dithiolated monomer (2,2′-(ethylenedioxy)diethane thiol, EDDET) and a diallylic monomer ((+)-*N,N′*-diallyltartramide, DATD) with UV radiation. Moreover, to achieve hydrogels with enhanced rheological properties, a triallylic monomer (1,3,5-triallyl-1,3,5-triazine-2,4,6(1H,3H,5H)-trione, TC) was added as a crosslinking agent. Different crosslinking degrees and chitosan/polymer proportions were proposed to evaluate the influence of both variables on rheological and microstructural properties of the resulting hydrogels.

2. Experimental

2.1. Materials

Low-molecular-weight chitosan (CTS, 130,000 g.mol^{-1}) with a deacetylation degree between 75 and 85 % was purchased from Sigma-Aldrich S.A. (Taufkirchen, Germany). An acetic acid solution of 0.05 M concentration and pH ~ 3.2 was used as polymerization solvent. For the click reaction, 2,2′-(ethylenedioxy)diethanethiol (EDDET), (+)-*N,N′*-diallyltartramide (DATD) and 1,3,5-triallyl-1,3,5-triazine-2,4,6(1H,3H,5H)-trione (TC) were used as the dithiolated monomer, diallylic monomer and crosslinking agent, respectively. All these reagents were provided by Sigma-Aldrich S.A. (Taufkirchen, Germany). 2,2-Dimethoxy-2-phenylacetophenone (DMPA) was used as the photo initiator agent of the polymerization reactions. It was purchased from Acros Organics (Geel, Belgium).

2.2. Hydrogels preparation

2.2.1. Photo-initiated click reactions

The proposed click reaction for hydrogel formation (Fig. 2) was carried out in non-inert conditions, with a slight excess of thiol groups (5 %) to neutralize the potential formation of hydroperoxyl radicals (HOO•) during the reaction process.

As was previously described, DATD and EDDET react with each other by means of a step polymerization procedure photoinitiated by DMPA (UV light, λ = 365 nm, P = 180 W) to form linear polymeric segments within the 3D-framework (Fig. 2). The three-dimensionality of the structure was achieved by the addition of a trifunctional crosslinker (TC) within the solution of CTS.

2.2.2. Semi-IPNs formation

For the preparation of semi-IPN hydrogels, the biopolymer used in all the trials was CTS (dissolved in a 0.05 M acetic acid solution at a final 3 wt % concentration) due to its outstanding properties mentioned above. The synthetic polymer chains will grow and crosslink within the CTS chain solution to improve the final mechanical and structural properties of the CTS solution. Thus, once the solution of CTS (3 wt %) was prepared, predetermined mmoles of DATD, EDDET and TC (the two later dissolved in ethanol) were subsequently added, and the mixture was stirred for five minutes to promote the homogenization of the sample. The amount of the reagents was calculated to meet the target CTS/polymer weight/weight ratios and crosslinking degrees (CD) (Table 1). Next, a solution of 10 % w/v of the photo-initiator (DMPA) in ethanol was added to the CTS suspension under dark conditions. The formation of the crosslinked network is conducted under UV light (λ = 365 nm, P = 180 W, 5 min) to yield the final CTS-based semi-IPN hydrogels. A schematic overview of the synthesis is shown in Fig. S1.

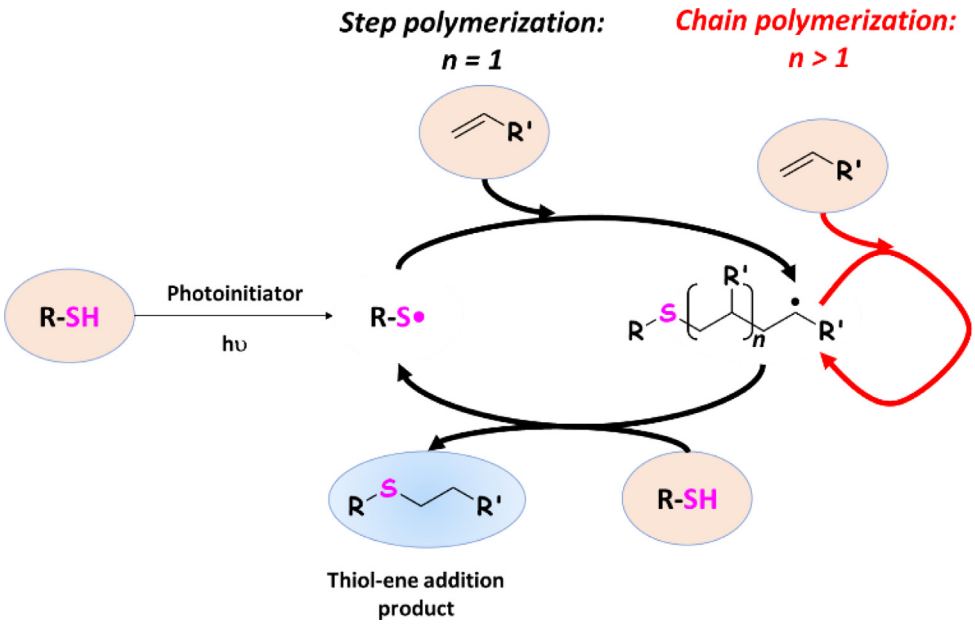

Fig. 1. Photoinitiated thiol-ene radical addition reaction mechanisms.

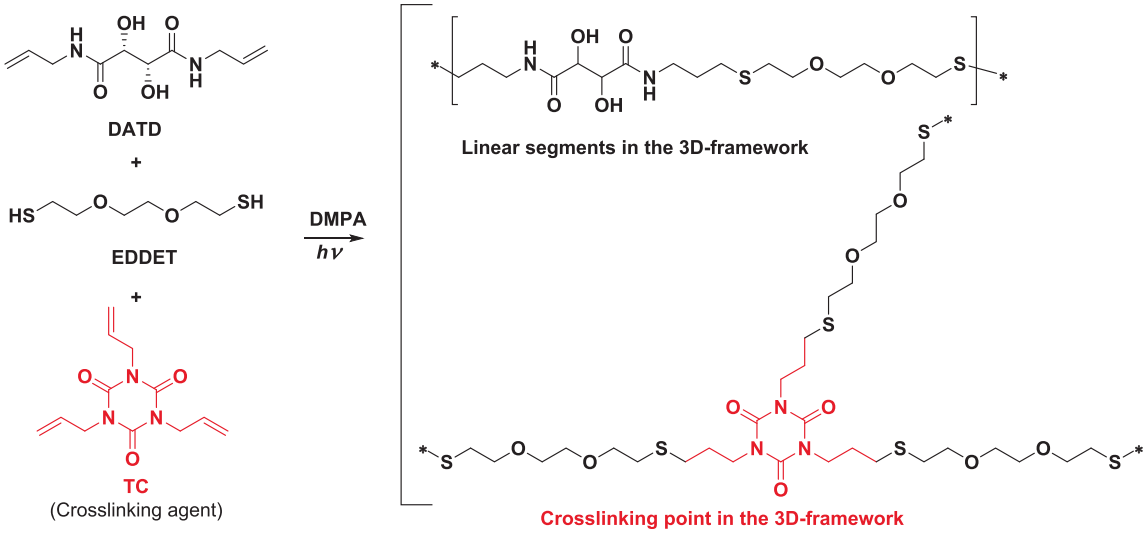

Fig. 2. Three-dimensional framework formation reaction by click thiol-ene photopolymerization.

Table 1
Systems proposed to evaluate the influence of both CD and polymers ratio on the resulting hydrogels.

Systems	CTS/Polymer ratio	CD (%)	DATD (mg|μmol)	TC (mg|μmol)	EDDET (mg|μmol)	DMPA (mL|μmol)
1	2/1	4	40.8|179	1.24|4.97	35.6|196	0.1|37.24
2	2/1	8	39.1|171	2.47|9.91	35.6|196	0.1|37.24
3	2/1	12	37.4|164	3.69|14.8	35.6|196	0.1|37.24
4	1/1	4	81.6|358	2.47|9.91	71.3|391	0.1|37.24
5	1/1	8	78.2|343	4.95|19.8	71.3|391	0.1|37.24
6	1/1	8	78.2|343	4.95|19.8	71.3|391	0.1|37.24
7	1/1	12	74.8|328	7.41|29.7	71.3|391	0.1|37.24
8	1/2	4	163|714	4.94|19.8	143|782	0.2|74.48
9	1/2	8	156|683	9.88|39.6	143|782	0.2|74.48
10	1/2	12	150|655	14.8|59.4	143|782	0.2|74.48

CTS: chitosan; CD: crosslinking degree; DATD: (+)-*N,N′*-diallyltartramide; TC: 1,3,5-triallyl-1,3,5-triazine-2,4,6(1H,3H,5H)-trione; EDDET: 2,2′-(ethylenedioxy)diethanethiol; DMPA: 2,2-Dimethoxy-2-phenylacetophenone.

As was previously indicated, two variables were studied to assess their influence on the properties of the resulting hydrogels, namely crosslinking degrees (CDs) (4, 8 and 12 %) and chitosan/polymer ratios (2/1, 1/1 and 1/2). The CD was set by a predetermined molar addition of the covalent crosslinker TC. Thus, the necessary amount of triallyl TC crosslinker was added so that, for example, 8 % of the thiol moieties of monomer EDDET would react with the crosslinker and the 92 % of the remaining thiol groups would couple with the diallyl monomer DATD. As a summary, the proposed systems are collected in Table 1. It is worth to mention that a duplicate of the intermediate system is necessary for the model design analysis so, for that reason, systems 5 and 6 are the same.

2.3. Hydrogels characterization

Once the semi-IPN hydrogel systems were formed, a rheological analysis was performed to characterize the rheological properties of each system and then, the evaluation of both chemical and morphological properties was carried out.

2.3.1. Rheological characterization

Rheological properties of the hydrogels were determined in an AR 2000 oscillatory rheometer (TA Instruments, New Castle, DE, USA) with parallel serrated plate geometry (diameter: 40 mm) by performing different rheological shear tests. Three types of rheological tests were performed:

- **Strain sweep tests**: Measurements between 10E and 4 and 0.1 % strain at a constant frequency of 1 Hz and 25 °C were performed to determine the linear viscoelastic range (interval where the elastic and viscous moduli are independent of the applied strain) and the critical strain (the maximum strain supported by the sample within the linear viscoelastic range).
- **Time sweep tests**: These tests were performed in the linear viscoelastic range, at constant frequency (1 Hz), strain (0.25 %) and temperature (25 °C) for 10 min (600 s). These tests allowed evaluating the evolution of the system with time, representing both G′ and G″ versus time.
- **Frequency sweep tests**: In this case, the measurements were carried out in a frequency range between 0.1 and 10 Hz at a constant strain within the linear viscoelastic range (0.25 %) and 25 °C. In these tests, the elastic and viscous moduli (G′ and G", respectively) were obtained, together with the loss tangent ($\tan\delta = G''/G'$) and complex viscosity ($\eta^* = ((G')^2 + (G'')^2)^{1/2}$). Furthermore, the values for G′, tanδ and η^* at 1 Hz (G'_1, $\tan(\delta)_1$ and η^*_1) were selected and tabulated to improve the comparison of the properties of the different systems.

2.3.2. Experimental model design for the analysis of rheological parameters

The operating conditions on the effect of the studied variables on the rheological and microstructural properties of the resulting hydrogels should have an influence. Therefore, different authors have studied different parameters levels [21,22].

A 23-1 Full factorial design (Table 2) was used to examine the influence of the independent operational variables on the resulting hydrogels. A total of 10 experiments were required for our considered independent variables at three levels. The values of independent variables were normalized from −1 to +1 using Eq. (1) in order to facilitate direct comparison of the coefficients and visualization of the effects of the individual independent variables on the response variable

$$X_n = \frac{X - \bar{X}}{\left\lfloor \frac{(X_{max} - X_{min})}{2} \right\rfloor} \quad (1)$$

Where x_n denotes the normalized value of independent variables; x is the obtained experimental value of the independent variable concerned; $\bar{X}$ is the mean of the experimental values for this independent variable in question; and x_{max} and x_{min} are the maximum and minimum values, respectively, of the independent variable.

2.3.3. Chemical characterization

The chemical structures of the IPNs were analysed by Fourier-Transform Infrared Spectroscopy (FTIR), using a Hyperion 1000 spectrophotometer (Bruker, Santa Clara, CA, USA). The samples were placed in an ATR diamond sensor to obtain their infrared profile. The measurements were obtained between 4500 and 600 cm^{-1} with an opening of 4 cm^{-1} and an acquisition of 200 scans. Baseline correction was performed by measuring without sample.

2.3.4. Microstructural characterization

Hydrogels were morphologically assessed using a cryo-scanning electron microscope (Cryo-SEM) Zeiss EVO (Stuttgart, Germany) at an acceleration voltage of 10 kV. The samples were previously cooled with liquid nitrogen and covered with a thin film of Au in a high-resolution sputter coater Leica (Wetzlar, Germany). A digital processing free software, FIJI Image-J (National Institutes of Health, Bethesda, MD, USA), was used to determine the mean pore size and general porosity of the selected hydrogels.

Table 2
Elastic modulus, loss tangent and complex viscosity measures at 1 Hz of semi-IPN hydrogels of chitosan and click polymer with CTS/polymer ratios of 2/1, 1/1 and 1/2 and different crosslinking degrees (4, 8 and 12 %). Different letters (a–b; A–D; α–δ) as superscripts were included to denote significant differences in the values shown in each column ($p < 0.05$).

Systems	Chitosan/Polymer ratio (CTS)	CD (%)	CTS[1]	CD[1]	G'_1 (Pa)	$\tan(\delta)_1$	$\lvert\eta^*_1\rvert$ (Pa·s)
1	2/1	4	−1	−1	8.52^{a}	0.47^{A}	126^{α}
2	2/1	8	−1	0	120^{b}	0.16^{B}	264^{β}
3	2/1	12	−1	1	20.3^{c}	0.29^{C}	197^{γ}
4	1/1	4	0	−1	10.4^{a}	0.40^{A}	$145^{\alpha,\gamma}$
5	1/1	8	0	0	474^{d}	0.15^{B}	585^{δ}
6	1/1	8	0	0	483^{d}	0.15^{B}	602^{δ}
7	1/1	12	0	1	139^{e}	0.12^{D}	$335^{\beta,\varepsilon}$
8	1/2	4	1	−1	61.2^{f}	0.19^{B}	$141^{\alpha,\beta}$
9	1/2	8	1	0	241^{g}	$0.14^{B,D}$	428^{ε}
10	1/2	12	1	1	94.9^{h}	0.15^{B}	299^{β}

[1] Normalized values of the independent variables.

2.4. Statistical analyses

At least three replicates were carried out for each measurement. Statistical analyses were performed with *t*-tests and one-way analysis of variance ($p < 0.05$), using PASW Statistics for Windows (Version18: SPSS Inc., Endecott, NY, USA). Standard deviations were calculated for selected parameters. The significant differences were established with a confidence level of 95 % ($p < 0.05$), which are indicated with different letters in the different tables.

3. Results and discussion

3.1. Rheological evaluation

3.1.1. Evaluation of the reaction and the influence of UV illumination. Crosslinking degree on the rheological properties of semi-IPN hydrogels

The evaluation of the reaction was studied by time sweep tests at different conditions (with and without UV radiation). As it can be seen in Fig. 3, two different effects occurred. On the one hand, the system measured with no radiation showed G″ values above G′ ones, which means that no gelification process took place. On the other hand, when the selected 1/1 CTS/polymer hydrogel with a crosslinking degree of 12 % (sample 7, chosen as reference for this assay) was subjected to UV radiation, the opposite effect was observed, as G′ values were higher than G″ ones from the beginning. This proves the instantaneous formation of the hydrogel, as the elastic modulus is above viscous modulus since the beginning of the assay and that UV radiation seems mandatory for the formation of the semi-IPN hydrogels. In addition, a slight increase of the elastic modulus can be observed along the whole test, which means that the structure keeps reinforcing when illuminated with UV radiation, though at a significantly slower pace.

3.1.2. Evaluation of the influence of crosslinking degree and CTS/polymer ratio on the rheological properties of semi-IPN hydrogels

For the analysis of the influence of CD on the rheological properties of the hydrogels, time sweep tests were conducted to assess the development of the gelation process of each system by the evolution of both elastic and viscous moduli with time (Fig. S2). In addition, a solution of pure chitosan (CTS) was analyzed as a reference.

Regarding CTS results, it can be noted that no hydrogel was formed, as the viscous modulus was above the elastic modulus throughout the entire test, which denotes a predominantly liquid behavior. Conversely, all other systems showed the characteristic behavior of hydrogels, with G′ above G″. Therefore, this demonstrated that chitosan cannot undergo gelation processes by itself, requiring a physical stimulus, as has been previously described in other works [34], or a chemical reaction in order to achieve a certain structuration degree [35,36]. It is clear that, with the proposed click reaction, even with the lowest CD, the structuration, and thus, the formation of semi-IPN hydrogels took place successfully and immediately for each chitosan/polymer ratio, regardless of the strength of the resulting hydrogels. The same behavior was observed in every chitosan/polymer ratio when CD was modified, where with 4 % CD, the obtained hydrogels seemed to be very weak, with G′ values close to G″ values. However, increasing CD led to a notorious increase of the elastic modulus, at least up to 8 % CD, since, as can be observed in Fig. S2, increasing CD even further does not necessarily entail an improvement of rheological properties. In fact, an excess amount of the thiolated compound may impair the ability for orthogonal crosslinking, conversely resulting in a reduced stiffness in the corresponding hydrogel, as proved by Muñoz et al. [37].

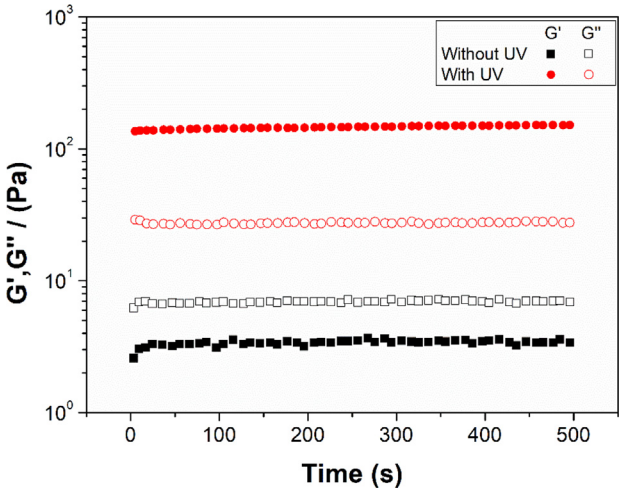

Fig. 3. Time sweep tests of 1/1 CTS/polymer ratio semi-IPN hydrogels with and without UV illumination.

For a further assessment, strain and frequency sweep tests were carried out to delve into the rheological characterization of the systems. The same tendency observed in the previous analyses can be observed in Fig. 4, where click reaction was required for the gelation process to occur, and increasing CD up to 8 % was beneficial for rheological properties, although a further increase was detrimental to the latter.

As can be observed, the systems had an increasing stabilization when increasing the CD, obtaining higher values of viscoelastic properties. However, all the hydrogels showed a similar critical strain (0.02 %) (Fig. 4A, 4C and 4E) when the structure started to break. The results of frequency sweep tests show values of elastic modulus (G') much higher than those of viscous modulus (G″), although they have a cutoff point at high frequencies, which are more evident at lower CD. In addition, the systems were not as stable with frequency, although they tended to of stabilize with increasing CD. Nevertheless, these results allowed us to confirm the formation of semi-IPN hydrogels with the proposed click reaction resulting in viscoelastic hydrogels whose stabilization depends on the extent of the crosslinking.

Moreover, it can be observed that, when the chitosan proportion was predominant (2/1) (Fig. 4A), the stability to strain was slightly worse compared to that of the 1/1 (Fig. 4C) and 1/2 (Fig. 4E systems and the same effect can be observed in the frequency sweep test (Fig. 4B, 4D and 4F), where structures of CD 4 and 12 % with 2/1 chitosan/polymer ratio (Fig. 4B) broke at frequencies from 4 Hz, approximately. However, compared to the mentioned systems, structures of the hydrogels with the same CD of 1/1 were not broken (Fig. 4D), whereas systems of 1/2 CTS/polymer ratio were more stable than the others. This fact confirmed that a higher presence of the click polymer produces a better formation and stabilization of the semi-IPN hydrogels' structures, leading to better rheological properties than the 2/1 systems, but not better than those of the ones obtained for the 1/1 systems.

For a better comparison, the values of elastic modulus, loss tangent and complex viscosity at 1 Hz (G'_1, $\tan(\delta)_1$ and η^*_1) are shown in Table 2. With the data in Table 2, it is easier to see that the system with the best rheological properties would apparently be 8 % with 1/1 CTS/polymer ratio, as it had the highest values of G'_1 and η^*_1 and a loss tangent close to 0.1. This is important, since the smaller the loss tangent value, the stronger the hydrogel, as was stated by Clark [38].

For each CTS/polymer ratio, it is proved that a CD of 8 % offers the best rheological properties and, comparing them, the system

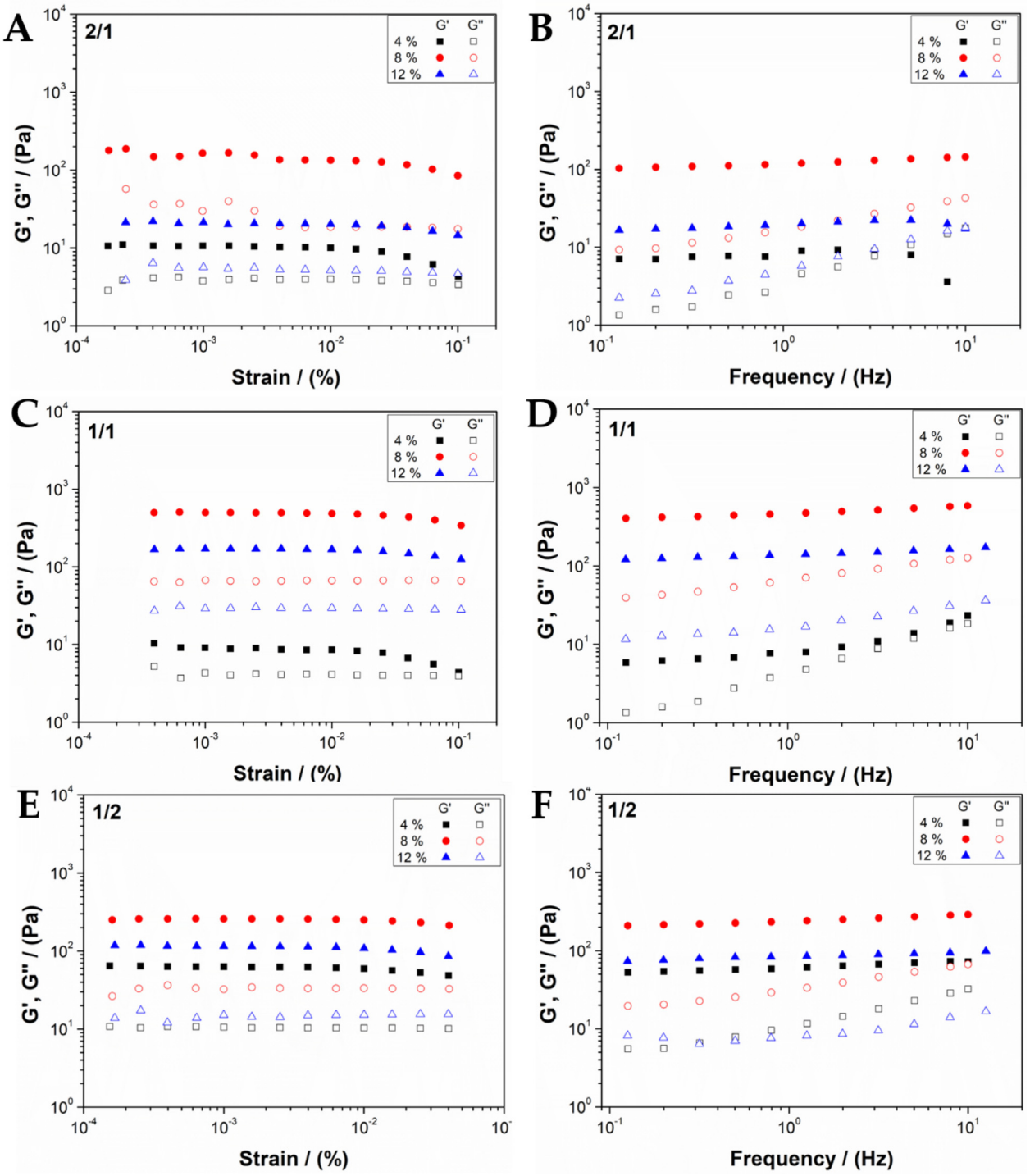

Fig. 4. Strain sweep (A, C, E) and frequency sweep (B, D, F) tests of 2/1, 1/1 and 1/2 CTS/polymer ratio semi-IPN hydrogels with different CDs (4, 8 and 12 %).

with a higher proportion of CTS (2/1) had the lowest value of G'_1 and η^*_1, although no significant variations were found for tan $(\delta)_1$. Besides, the systems with 2/1 CTS/polymer ratio showed worse values of the studied rheological properties, when comparing the same CDs of the other systems, indicating lower values of elastic modulus and complex viscosity, with a loss tangent over 0.2 in 4 and 12 % cases, respectively, assuming a less resistant behavior, as was previously described. On the other hand, the systems with a higher proportion of click polymer (1/2) displayed improvements and deteriorations with respect to the 1/1 systems, inasmuch as in hydrogels with 4 % CD, the 1/2 systems exhibited better elastic modulus and loss tangent values and no significant variations in complex viscosity. Nevertheless, when comparing systems with CDs of 8 and 12 %, the 1/1 CTS/polymer ratio systems had better rheological properties. This could be due, to the previously mentioned effect of the concentration of the thiolated compound demonstrated by Muñoz et al. [37], who indicated that an excess amount of the thiolated compound impaired the ability for orthogonal crosslinking, resulting in a reduced stiffness in the corresponding hydrogels. As long as the 1/2 systems had a higher proportion of click polymer and, therefore, a higher concentration of every reagent involved in the click reaction, it could be assumed

that, with low CDs (4 %), the higher presence of the click polymer effect prevails over the concentration of thiolated compound, leading to better rheological properties than those of the 1/1 systems. Moreover, even though the values of mechanical properties increased by using 8 % CD, following the tendency observed throughout this study, these properties did not even reach the values obtained for G'_1 and η^*_1 for 8 % 1/1. This would confirm that, from this point, the effect of the concentration of thiolated groups would start to prevail.

3.1.3. Correlations of rheological parameters with CTS/polymer ratio and CD based on an experimental model design

Quantifying the relative effects of the independent variables on the dependent variables in the found equations is somewhat difficult, since both contain complex terms involving interactions between independent variables (Table 3). Consequently, Figs. 5 and 6 show the evolution of each dependent variable studied, as a function of each independent variable constructed from the calculated equations.

In this regard, if the independent variable studied had a slight effect on the dependent variable under consideration, then the slope of the curve (at different levels of the independent variables) would be low. On the other hand, if the independent variable studied had (at a given level of the other independent variable) a high level of influence, the slope of the corresponding curve would be accordingly high.

As can be observed in Fig. 5, CTS exhibits a slightly greater influence on G'_1 than that found for CD, while the quadratic terms cause the influence to be predominantly exponential for both variables. Accordingly, minimum values of G'_1 at the extreme values of these two variables can be found. On the contrary, a maximum value of G'_1 for the intermediate values of the two studied variables can be calculated.

Furthermore, Fig. 6 shows that the negative influence of CTS (lower values) on $\tan(\delta)_1$ is similar (at the concentrations studied) among the systems and independent of the CD values. Nevertheless, a statistical dependence of the CD levels on the $\tan(\delta)_1$ values was found. In this way, low $\tan_{\delta 1Hz}$ values under high CTS conditions (due to the negative influence stated above) and intermediate or high CD values can be found. Furthermore, as CD levels decreased, the $\tan(\delta)_1$ values found increased significantly and higher values of $\tan(\delta)_1$ under lower levels of both CD and CTS were observed.

3.2. Chemical evaluation

Once the rheological characterization was finished, hydrogels were selected, specifically the ones with 8 % CD for all the CTS/polymer ratios evaluated, to further assess the reaction course and the formation of the framework, taking these hydrogels as representative of each ratio. Thus, ATR-FTIR measurements were carried out (Fig. 7) to analyze the chemical structure of each system and to prove the formation of the click polymer, as well as the influence of varying the polymers proportions.

Table 3
Yielded equations and statistical parameters for each studied (dependent) variable.

Equations	p	F	R^2
G'_1 = 436.721–81.794 CTS − 242.307 CTS^2 − 271.022 CD^2	0.0052	34.09	0.978
$\tan(\delta)_1$ = 0.1275–0.0783 CTS − 0.0750CD + 0.1341 CD^2	0.0055	12.37	0.951

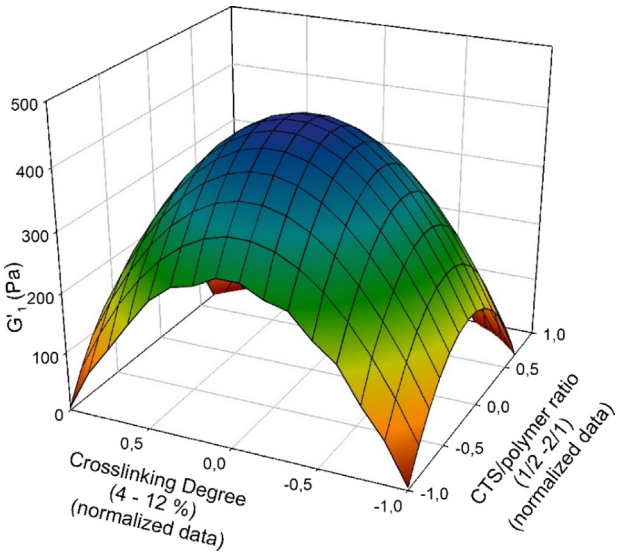

Fig. 5. Response surface for G'_1 as dependent variable with respect to crosslinking degree (CD) and CTS.

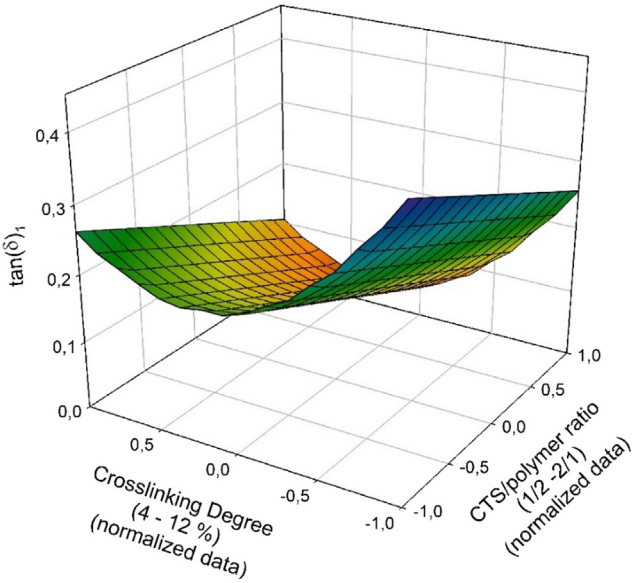

Fig. 6. Response surface for tan(δ)1 as dependent variable with respect to CD and CTS.

Fig. 7A depicts the FTIR spectra of CTS, DATD and the selected 8 % 1/1 CTS/polymer hydrogel. With these data, it is possible to demonstrate the formation of the new polymeric chain *via* thiolene reaction promoted with UV radiation and, thus, the formation of the IPN hydrogel. The most determinant fact that proves that the click reaction has taken place is the disappearance of the characteristic peaks of allylic moieties in the IPN system. Therefore, the characteristic bands of allylic compounds found in the DATD monomer spectrum (=CHst at 3011 cm^{-1} and =CHδ oop at 985 and 915 cm^{-1}) are missing in the spectrum of the IPN hydrogel, which corroborates the success of the polymerization reaction [39]. It can also be observed in the DATD spectrum that the characteristic and well-defined N—H and O—H stretching bands (N—H at 3314 cm^{-1} and O—H at 3211 cm^{-1}) collapsed in the spectrum of the IPN into a broader band that includes not only the

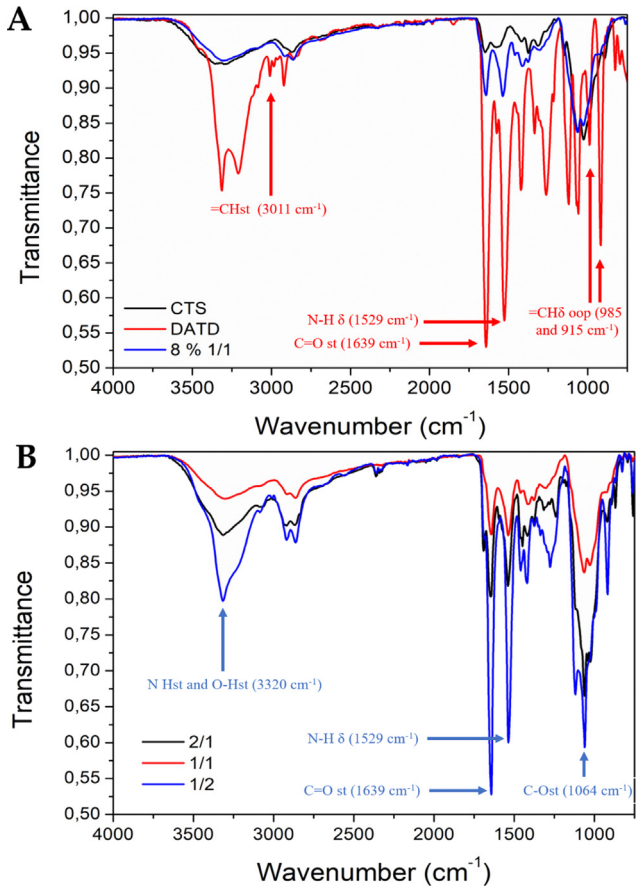

Fig. 7. (A) ATR-FTIR spectra of CTS and DATD (reagents) and selected semi-IPN hydrogel system. (B) Comparison of the ATR-FTIR spectra of the representative 2/1 (black), 1/1 (red) and 1/2 (blue) CTS/polymer ratio systems. (For interpretation of the references to colour in this figure legend, the reader is referred to the web version of this article.)

bands already mentioned, but also those that can be correlated to the N—H and O—H bonds from CTS. Moreover, the intensity of the amide I and amide II bands (C═O st at 1639 cm^{-1} and N—H δ at 1529 cm^{-1}) of the IPN system increased compared to the CTS bands due to the addition of the novel click polymer.

The comparison between the representative systems for each CTS/polymer ratio (Fig. 7B) proves that, when increasing the ratio of the click polymer in detriment of CTS, an increase in the bands associated with the synthetic polymer is found. Thus, for example, the intensity of characteristic bands such as C-Ost from the DATD C—OH moieties (1064 cm^{-1}), amide I and amide II (1640 and 1536 cm^{-1}) and the wide band of N—Hst and O-Hst (3320 cm^{-1}) were higher when comparing the 1/2 (blue) system with the rest of the systems [39].

3.3. Microstructural evaluation

Fig. 8 shows a view of the selected hydrogels as references, both at a macroscopic and microscopic scale. Regarding the macroscopic appearance, hydrogels were obtained with an appearance similar to that obtained in other studies where IPN hydrogels were synthesized with crosslinking based on a click-type reaction [40]. No appreciable differences were observed at a macroscopical level. On the other hand, when studying the microscopical structure, it can be observed that each hydrogel presents a completely different structure. Firstly, the structure of the 8 % CD with 2/1 CTS/polymer ratio hydrogel (Fig. 8A') displays a very heterogeneous structure, due to its notable difference in not only pore size (mean pore size = 33.01 ± 40.33 um) but also pore distribution. This structure is characterized by its high porosity, going from very small, rounded pores to large oval pores. Moreover, some tiny fibers can be observed in several pores, forming smaller pores. On the other hand, Fig. 8B' shows the structure obtained for the hydrogel with 8 % CD and 1/1 CTS/polymer ratio, which can be described as a leaf-like structure, with also high porosity, but with a much more homogeneous pore distribution and size (36.89 ± 3.11 um), compared to the one shown in Fig. 8A'. Finally, the structure depicted in Fig. 8C', which corresponds to the 8 % CD with 1/2 CTS/polymer ratio hydrogel, could be described as an intermediate structure between the previous ones, with a homogeneous pore distribution and size, but presenting several oval pores, similar to those observed on the structure of the 2/1 hydrogel, but with smaller size (20.51 ± 10.53 um). Comparing these structures between them and with the results obtained in the previous analyses, it can be established that increasing the click polymer concentration, and thus its presence in the structure, leads to a leaf-like structure with much more homogeneous pores in the case of the 1/1 system, which could possibly explain the better rheological properties obtained compared to the rest of the systems. The representative system of the 1/2 ratio was proved to have the greatest amount of click polymer (Fig. 7B); however, as can be noted, this does not necessarily mean the best for the semi-IPN system, as its structure has been described as an intermediate structure between the other ones (Fig. 8C'). In addition, it is worth to mention that, even though the mean pore size of 2/1 system (33.01 ± 40.33 um) would apparently be smaller than the one of 1/1 reference system (36.89 ± 3.11 um), this would be due to the quantification of both small rounded and the large oval pores in the 2/1 system, resulting in the obtained average.

The resulting rheological properties fit with the structure obtained, as they were intermediate when comparing the results obtained for the representative systems of the 2/1 and 1/1 ratios. The poor properties obtained for the 2/1 systems can be attributed to the structures obtained for the representative system of this ratio, specifically due to the observed larger pores observed in Fig. 8A', which were detrimental, particularly to the rheological properties. Nevertheless, the obtained porosity data of each representative system, which were 62.97 ± 2.60, 63.43 ± 3.43 and 64.83 ± 4.75 for 2/1, 1/1 and 1/2 systems, respectively, did not show significant differences between them. However, these porosity values would be suitable for biomedical applications as they are located between the suitable porosity range for cell adhesion and proliferation, according to Vannozzi et al. (2017) [41]. Thus, these systems could be of interests for conducting experiments in future works, in order to test their viability for applications such as tissue engineering, controlled drug delivery, wound healing or bioprinting.

Compared to results obtained in previous studies, the implementation of a photoinitiated click reaction in order to obtained chitosan-based systems is a promising alternative to attain hydrogels for biomedical applications, as most of the candidates evaluated in this work had similar or better rheological and microstructural properties compared to chitosan-based hydrogels blended with collagen [42] or dual ionically-crosslinked with poly(NIPAm-co-AMPS) [43]. Nevertheless, there is still much more research needed for this alternative to improve the performance of chitosan-based hydrogels [34,44,45]. Using different conditions or other monomers who could lead to more resistant polymeric chains would be interesting paths to follow.

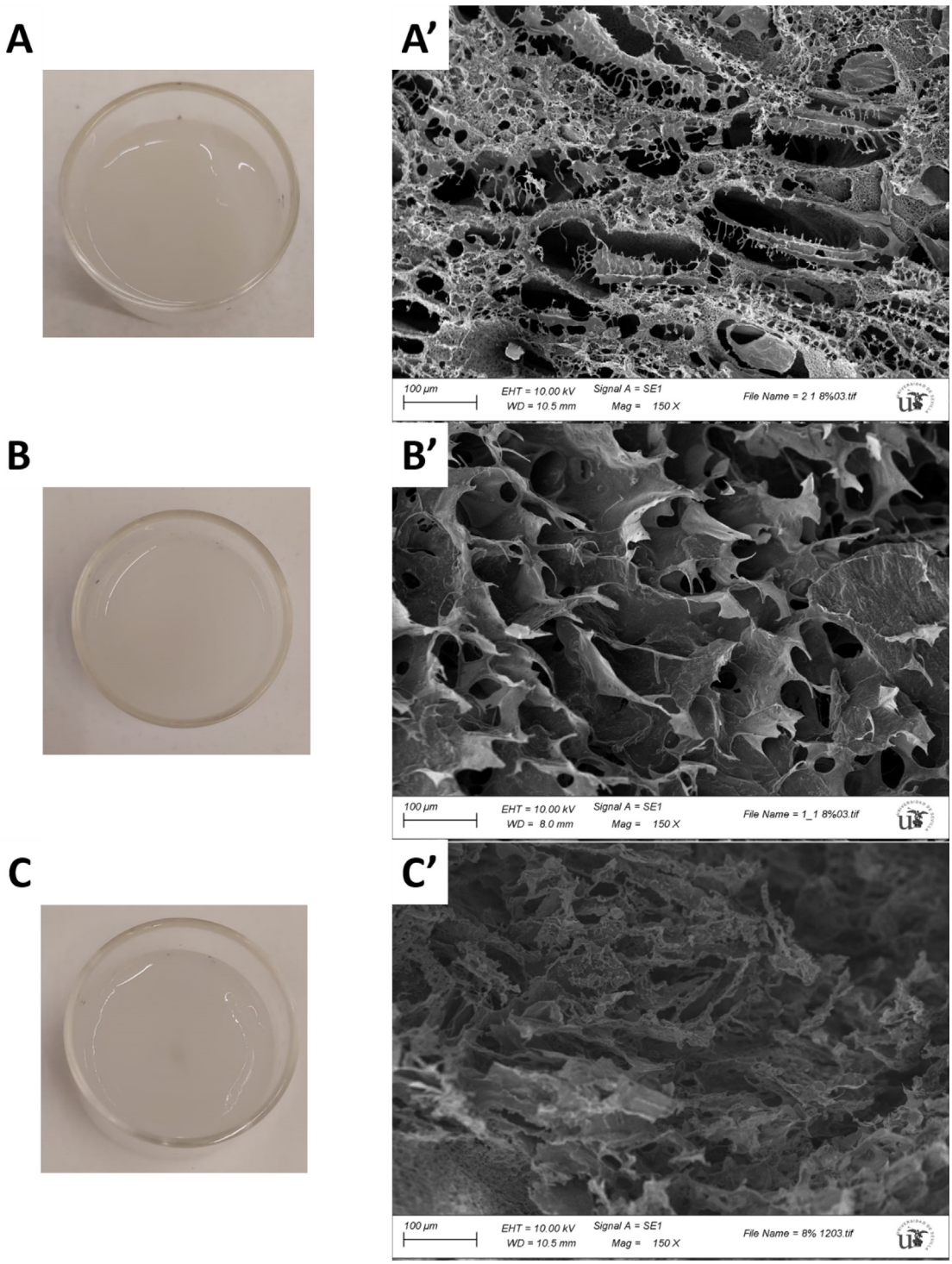

Fig. 8. Macroscopic (A, B and C) and SEM images (A', B' and C') of the representative systems of the different CTS/polymer ratios studied, namely 2/1, 1/1 and 1/2, respectively.

4. Conclusions

Novel semi-IPN hydrogels based on chitosan and a polymer synthesized by a thiol-ene photoinitiated click reaction were successfully developed. Rheological characterization revealed the influence of both crosslinking degree and polymers ratio on the resulting hydrogels' properties. Increasing CD from 4 to 8 % led to an improvement of every analyzed rheological property, although further increase in the CD was detrimental. The most probable reason for these findings is related to the increase in the thiolated monomer compared to the allylic monomer when the degree of crosslinking was raised, resulting in the formation of stiffest nodules with reduced wettability, which hampered gel formation. This tendency was observed in every CTS/polymer ratio analyzed.

On the other hand, the variation of CTS/polymer ratio resulted in a tendency similar to the one observed for the variation of CD, as 2/1 systems (the ones with a smaller amount of click polymer) displayed the worst rheological properties for each CD compared to the rest, probably due to the scant amount of interpenetrated

polymer responsible for the improvement of the rheological properties in the other systems. Its heterogeneous structure, which contained some large pores, impaired its rheological behavior. When click polymer proportion was increased to 1/1, the best rheological performance was achieved, according to a leaf-like and porous structure, with a homogeneous distribution of pore size. However, when click polymer amount was increased to 1/2, once again, the rheological properties were hindered, obtaining intermediate values and a structure that displayed similarities with the structures obtained for the other ratios evaluated. This analysis allowed establishing that the system with the best and most suitable properties was 1/1 and 8 % CD.

Consequently, this work demonstrates that the formation of semi-IPN systems by thiol-ene click reactions can have a substantial impact on the mechanical and rheological properties of natural and semisynthetic biopolymers, specifically in CTS systems. This study paves the road for future work, where the suitability of these systems for different applications, such as tissue engineering, drug delivery systems or 3D-printing, will be tested.

Funding

This study was financially supported by MCIN/AEI/10.13039/501100011033/FEDER, UE, through the project PID2021-124294OB-C21. The authors gratefully acknowledge their financial support. This work was also possible thanks to the postdoctoral contract of Víctor M. Pérez Puyana from the "Contratación de Personal Investigador Doctor" supported by the European Social Fund and Junta de Andalucía (PAIDI DOCTOR – Convocatoria 2019–2020, DOC_00586).

Author contributions

Conceptualization, P.S.-C., A.R., M.-V.P, V.P.-P.; methodology, P. S.-C., M.-V.P, V.P.-P.; validation, A.R., M.J.D., M.-V.P, V.P.-P.; formal analysis, P.S.-C., M.J.D., V.P.-P.; investigation, P.S.-C.; resources, A. R., M.-V.P, V.P.-P.; data curation, P.S.-C., M.J.D.; writing, P.S.-C., M. J.D., M.-V.P, V.P.-P.; visualization, P.S.-C.; supervision, A.R., M.J.D., M.-V.P, V.P.-P.; project administration, V.P.-P.; funding acquisition, A.R, V.P.-P. All authors have read and agreed to the published version of the manuscript.

Data availability

Data will be made available on request.

Declaration of Competing Interest

The authors declare that they have no known competing financial interests or personal relationships that could have appeared to influence the work reported in this paper.

Acknowledgements

Authors want to acknowledge CITIUS for granting access to and their assistance with the Microscopy service.

Appendix A. Supplementary data

Supplementary data to this article can be found online at https://doi.org/10.1016/j.molliq.2023.121735.

References

[1] A.S. Hoffman, Hydrogels for biomedical applications, Adv. Drug Deliv. Rev. 64 (2012) 18–23, https://doi.org/10.1016/j.addr.2012.09.010.
[2] M.L. Pita-López, G. Fletes-Vargas, H. Espinosa-Andrews, R. Rodríguez-Rodríguez, Physically cross-linked chitosan-based hydrogels for tissue engineering applications: a state-of-the-art review, Eur. Polym. J. 145 (2021), https://doi.org/10.1016/j.eurpolymj.2020.110176.
[3] Z. Liu, K. Wang, X. Peng, L. Zhang, Chitosan-based drug delivery systems: current strategic design and potential application in human hard tissue repair, Eur. Polym. J. 166 (2022), https://doi.org/10.1016/j.eurpolymj.2021.110979.
[4] W. Kalaithong, R. Molloy, K. Nalampang, R. Somsunan, Design and optimization of polymerization parameters of carboxymethyl chitosan and sodium 2-acrylamido-2-methylpropane sulfonate hydrogels as wound dressing materials, Eur. Polym. J. 143 (2021), https://doi.org/10.1016/j.eurpolymj.2020.110186.
[5] D. Noferini, A. Faraone, M. Rossi, E. Mamontov, E. Fratini, P. Baglioni, Disentangling polymer network and hydration water dynamics in polyhydroxyethyl methacrylate physical and chemical hydrogels, J. Phys. Chem. C 123 (2019) 19183–19194, https://doi.org/10.1021/acs.jpcc.9b04212.
[6] S. Chaudhary, E. Chakraborty, Hydrogel based tissue engineering and its future applications in personalized disease modeling and regenerative therapy, Beni-Suef Univ., J. Basic Appl. Sci. (2022) 1–15, https://doi.org/10.1186/s43088-021-00172-1.
[7] M.S. Kim, G.W. Oh, Y.M. Jang, S.C. Ko, W.S. Park, I.W. Choi, Y.M. Kim, W.K. Jung, Antimicrobial hydrogels based on PVA and diphlorethohydroxycarmalol (DPHC) derived from brown alga Ishige okamurae: an in vitro and in vivo study for wound dressing application, Mater. Sci. Eng. C 107 (2020), https://doi.org/10.1016/j.msec.2019.110352.
[8] P. Sánchez-Cid, M. Jiménez-Rosado, V. Perez-Puyana, A. Guerrero, A. Romero, Rheological and microstructural evaluation of collagen-based scaffolds crosslinked with fructose, Polymers (Basel) 13 (2021) 1–11, https://doi.org/10.3390/polym13040632.
[9] H. Chen, D. Wu, W. Ma, C. Wu, J. Liu, M. Du, Strong fish gelatin hydrogels double crosslinked by transglutaminase and carrageenan, Food Chem. 376 (2022), https://doi.org/10.1016/j.foodchem.2021.131873.
[10] H. Zhang, J. Cheng, Q. Ao, Preparation of alginate-based biomaterials and their applications in biomedicine, Mar. Drugs 19 (2021) 1–24, https://doi.org/10.3390/md19050264.
[11] P. Sánchez-Cid, M. Jiménez-Rosado, A. Romero, V. Pérez-Puyana, Novel trends in hydrogel development for biomedical applications: a review, Polymers (Basel) 14 (2022), https://doi.org/10.3390/polym14153023.
[12] A. Khan, K.A. Alamry, A.M. Asiri, Multifunctional Biopolymers-Based Composite Materials for Biomedical Applications: A Systematic Review, ChemistrySelect 6 (2021) 154–176, https://doi.org/10.1002/slct.202003978.
[13] E. Águila-Almanza, S.S. Low, H. Hernández-Cocoletzi, A. Atonal-Sandoval, E. Rubio-Rosas, J. Violante-González, P.L. Show, Facile and green approach in managing sand crab carapace biowaste for obtention of high deacetylation percentage chitosan, J. Environ. Chem. Eng. 9 (2021), https://doi.org/10.1016/j.jece.2021.105229.
[14] M.C.G. Pellá, M.K. Lima-Tenório, E.T. Tenório-Neto, M.R. Guilherme, E.C. Muniz, A.F. Rubira, Chitosan-based hydrogels: From preparation to biomedical applications, Carbohydr. Polym. 196 (2018) 233–245, https://doi.org/10.1016/j.carbpol.2018.05.033.
[15] A. Grząbka-Zasadzińska, T. Amietszajew, S. Borysiak, Thermal and mechanical properties of chitosan nanocomposites with cellulose modified in ionic liquids, J. Therm. Anal. Calorim. 130 (2017) 143–154, https://doi.org/10.1007/s10973-017-6295-3.
[16] J. Fu, F. Yang, Z. Guo, The chitosan hydrogels: from structure to function, New J. Chem. 42 (2018) 17162–17180, https://doi.org/10.1039/C8NJ03482F.
[17] Y. Dong, W. Hassan, Y. Zheng, A.O. Saeed, H. Cao, H. Tai, A. Pandit, W. Wang, Thermoresponsive hyperbranched copolymer with multi acrylate functionality for in situ cross-linkable hyaluronic acid composite semi-IPN hydrogel, J. Mater. Sci. - Mater. Med. 23 (2012) 25–35, https://doi.org/10.1007/s10856-011-4496-z.
[18] Y. Zhang, Z. Fan, C. Xu, S. Fang, X. Liu, X. Li, Tough biohydrogels with interpenetrating network structure by bienzymatic crosslinking approach, Eur. Polym. J. 72 (2015) 717–725, https://doi.org/10.1016/j.eurpolymj.2014.12.038.
[19] D. Myung, D. Waters, M. Wiseman, P.-E. Duhamel, J. Noolandi, C.N. Ta, C.W. Frank, Progress in the development of the interpenetrating polymer network hydrogels, Polym. Adv. Technol. (2008) 647–657, https://doi.org/10.1002/pat.
[20] E.S. Dragan, Design and applications of interpenetrating polymer network hydrogels. A review, Chem. Eng. J. 243 (2014) 572–590, https://doi.org/10.1016/j.cej.2014.01.065.
[21] S.J. Kim, S.G. Yoon, S.I. Kim, Synthesis and characteristics of interpenetrating polymer network hydrogels composed of alginate and poly (diallydimethylammonium chloride), J. Appl. Polym. Sci. 91 (2004) 3705–3709, https://doi.org/10.1002/app.13615.
[22] J.L. Aparicio-Collado, J.J. Novoa, J. Molina-Mateo, C. Torregrosa-Cabanilles, Á. Serrano-Aroca, R. Sabater I Serra, Novel semi-interpenetrated polymer networks of poly(3-hydroxybutyrate-co-3-hydroxyvalerate)/poly (vinyl alcohol) with incorporated conductive polypyrrole nanoparticles, Polymers (Basel) 13 (2021) 1–21, doi: 10.3390/polym13010057.

[23] H.C. Kolb, M.G. Finn, K.B. Sharpless, Click chemistry: diverse chemical function from a few good reactions, Angew. Chemie - Int. Ed. 40 (2001) 2004–2021, doi: 10.1002/1521-3773(20010601)40:11<2004::AID-ANIE2004>3.0.CO;2-5.
[24] X. Zuo, S. Wang, K. Zheng, C. Wu, D. Zhang, Z. Dong, T. Wang, F. Xu, J. Guo, Y. Yang, Fluorescent-brightener-mediated thiol-ene reactions under visible-light LED: A green and facile synthesis route to hyperbranched polymers and stimuli-sensitive nanoemulsions, Dye. Pigment. 189 (2021) 109253, doi: 10.1016/j.dyepig.2021.109253.
[25] C.E. Hoyle, C.N. Bowman, Thiol-ene click chemistry, Angew. Chemie - Int. Ed. 49 (2010) 1540–1573, https://doi.org/10.1002/anie.200903924.
[26] S. Wang, X. Ji, S. Chen, C. Zhang, Y. Wang, H. Lin, L. Zhao, Study of double-bonded carboxymethyl chitosan/cysteamine-modified chondroitin sulfate composite dressing for hemostatic application, Eur. Polym. J. 162 (2022), https://doi.org/10.1016/j.eurpolymj.2021.110875.
[27] S. Summonte, G.F. Racaniello, A. Lopedota, N. Denora, A. Bernkop-Schnürch, Thiolated polymeric hydrogels for biomedical application: cross-linking mechanisms, J. Control. Release 330 (2021) 470–482, https://doi.org/10.1016/j.jconrel.2020.12.037.
[28] A.B. Lowe, Thiol-ene "click" reactions and recent applications in polymer and materials synthesis, Polym. Chem. 1 (2010) 17–36, https://doi.org/10.1039/b9py00216b.
[29] S. Stichler, T. Jungst, M. Schamel, I. Zilkowski, M. Kuhlmann, T. Böck, T. Blunk, J. Teßmar, J. Groll, Thiol-ene clickable poly(glycidol) hydrogels for biofabrication, Ann. Biomed. Eng. 45 (2017) 273–285, https://doi.org/10.1007/s10439-016-1633-3.
[30] C. Leichner, M. Jelkmann, A. Bernkop-Schnürch, Thiolated polymers: bioinspired polymers utilizing one of the most important bridging structures in nature, Adv. Drug Deliv. Rev. 151–152 (2019) 191–221, https://doi.org/10.1016/j.addr.2019.04.007.
[31] R. Holmes, X. Bin Yang, A. Dunne, L. Florea, D. Wood, G. Tronci, Thiol-ene photo-click collagen-PEG hydrogels: impact of water-soluble photoinitiators on cell viability, gelation kinetics and rheological properties, Polymers (Basel) 9 (2017), https://doi.org/10.3390/polym9060226.
[32] N.B. Cramer, S.K. Reddy, A.K. O'Brien, C.N. Bowman, Thiol - ene photopolymerization mechanism and rate limiting step changes for various vinyl functional group chemistries, Macromolecules 36 (2003) 7964–7969, https://doi.org/10.1021/ma034667s.
[33] N.B. Cramer, C.N. Bowman, Kinetics of thiol-ene and thiol-acrylate photopolymerizations with real-time Fourier transform infrared, J. Polym. Sci. A Polym. Chem. 39 (2001) 3311–3319, https://doi.org/10.1002/pola.1314.
[34] P. Sánchez-Cid, M. Jiménez-Rosado, M. Alonso-González, A. Romero, V. Perez-Puyana, Applied rheology as tool for the assessment of chitosan hydrogels for regenerative medicine, Polymers (Basel) 13 (2021), https://doi.org/10.3390/polym13132189.
[35] N. Iglesias, E. Galbis, C. Valencia, M.J. Díaz-Blanco, B. Lacroix, M.V. de-Paz, Biodegradable double cross-linked chitosan hydrogels for drug delivery: Impact of chemistry on rheological and pharmacological performance, Int. J. Biol. Macromol. 165 (2020) 2205–2218, doi: 10.1016/j.ijbiomac.2020.10.006.
[36] N. Iglesias, E. Galbis, C. Valencia, M.V. de-Paz, J.A. Galbis, Reversible pH-sensitive chitosan-based hydrogels. Influence of dispersion composition on rheological properties and sustained drug delivery, Polymers (Basel) 10 (2018), doi: 10.3390/polym10040392.
[37] Z. Mũnoz, H. Shih, C.C. Lin, Gelatin hydrogels formed by orthogonal thiol-norbornene photochemistry for cell encapsulation, Biomater. Sci. 2 (2014) 1063–1072, https://doi.org/10.1039/c4bm00070f.
[38] A. Clark, Structural and Mechanical Properties of Biopolymer Gels, Woodhead, 1991, doi: 10.1533/9781845698331.322.
[39] E. Pretsch, P. Bühlmann, M. Badertscher, Structure Determination of Organic Compounds, fourth ed., Springer, Berlin, 2009, doi: 10.1007/978-3-540-93810-1.
[40] P. Wiwatsamphan, S. Chirachanchai, Persistently reversible pH-/thermo-responsive chitosan/poly (N-isopropyl acrylamide) hydrogel through clickable crosslinked interpenetrating network, Polym. Degrad. Stab. 198 (2022), https://doi.org/10.1016/j.polymdegradstab.2022.109874.
[41] L. Vannozzi, L. Ricotti, T. Santaniello, T. Terencio, R. Oropesa-Nunez, C. Canale, F. Borghi, A. Menciassi, C. Lenardi, I. Gerges, 3D porous polyurethanes featured by different mechanical properties: characterization and interaction with skeletal muscle cells, J. Mech. Behav. Biomed. Mater. 75 (2017) 147–159, https://doi.org/10.1016/j.jmbbm.2017.07.018.
[42] P. Sánchez-Cid, M. Jiménez-Rosado, J.F. Rubio-Valle, A. Romero, F.J. Ostos, R.E.I. Benhnia, V. Perez-Puyana, Biocompatible and thermoresistant hydrogels based on collagen and chitosan, Polymers (Basel) 14 (2022) 1–14, https://doi.org/10.3390/polym14020272.
[43] J. Zhao, L. Cui, X. Wang, C. Deng, Dual ionically crosslinked chitosan–based injectable hydrogel as drug delivery system, Colloid Polym. Sci. 300 (2022) 1075–1086, https://doi.org/10.1007/s00396-022-05003-y.
[44] F. Wahid, X.H. Hu, L.Q. Chu, S.R. Jia, Y.Y. Xie, C. Zhong, Development of bacterial cellulose/chitosan based semi-interpenetrating hydrogels with improved mechanical and antibacterial properties, Int. J. Biol. Macromol. 122 (2019) 380–387, https://doi.org/10.1016/j.ijbiomac.2018.10.105.
[45] S. Coşkun, S.O. Akbulut, B. Sarıkaya, S. Çakmak, M. Gümüşderelioğlu, Formulation of chitosan and chitosan-nanoHAp bioinks and investigation of printability with optimized bioprinting parameters, Int. J. Biol. Macromol. 222 (2022) 1453–1464, https://doi.org/10.1016/j.ijbiomac.2022.09.078.